Numerical and Experimental Investigation of a Cable-based Nonlinear Tuned Mass Damper to Reduce Free and Forced Vibrations

Diego A. Zamora-Garcia, Luis M. Acosta-Carrion, Mercedes X. Zepeda-Fuentes, Ma. Pilar Corona-Lira, Alejandro C. Ramirez-Reivich
School of Engineering, National Autonomous University of Mexico, Mexico City, Mexico
Email: zamoradazg7@hotmail.com, acostaluis1001@gmail.com, ximenazf42@gmail.com, pilicorona@comunidad.unam.mx, areivich@unam.mx

Abstract—**In this investigation the concept of the cable-based tuned mass damper (CB-TMD) is presented. This is an oscillator that presents geometric nonlinearities and has peculiar characteristics of elasticity and energy dissipation. Through numerical simulations and experimental procedures, it is evaluated as an attenuator of free vibrations and forced vibrations. It was found that this shock absorber does not have a good performance in reducing the settling time of free vibrations; however, it can reduce the amplitude of forced vibration in a range of frequencies.**

Index Terms—**Tuned mass damper, geometrically nonlinear systems, free vibrations, forced vibrations, nonlinear systems.**

I. Introduction

For most practical cases in engineering, vibration is an undesirable feature. This problem occurs both in large civil structures such as buildings and bridges, and in mechanical structures such as engines, mechanisms, robots, among others. In order to reduce vibration, various damping techniques have been developed. One of these methodologies is the tuned mass damper (TMD). Some solutions of tuned mass dampers for vibration attenuation have been proposed in the work of Gutierrez and Adeli [1]; a summary of some types of tuned mass dampers and their application in civil engineering can be observed. Other authors have analyzed the effect of a nonlinear spring on TMD [2]. And some have added the concept of energy harvest along with the TMD [3].

In general, tuned mass dampers have been widely studied and various solutions have been proposed for very particular cases. But most studies have been done for linear systems. It seems that, the influence of tuned mass dampers with non-linear characteristics in the attenuation of structural vibrations has been little studied. In the present investigation, a numerical and experimental study of the effectiveness of tuned mass dampers with nonlinearities in free and forced vibrations of a main structure with linear behavior was carried out.

Manuscript received November 14, 2019; revised August 20, 2020.

This work presents the concept of cable-based tuned mass damper (CB-TMD). This shock absorber design uses a planar arrangement of cables with a mass in the center. The idea comes from the configuration of planar cable robots. The mass has smaller dimensions with respect to the cables. The oscillation outside the plane of the cables has non-linear characteristics, this is due to the cables have an elongation and a change of direction, therefore, presents geometric nonlinearities. In a previous work it has been found that the characteristic behavior of this system is due to a low stiffness zone and a low energy dissipation zone centered on the equilibrium point [4]. The axial vibration of the cables has been modeled as Kelvin-Voight. Alternatively, this model has been experimentally validated and its elastic and viscous parameters have been defined as a function of length [5].

Some authors have studied viscoelastic TMD [6] and others have studied geometric nonlinearities analytically, in particular, geometrically nonlinear damping can be reviewed in [7] and [8]. It was difficult to replicate these types of systems in the physical world because viscous dampers based on cylinders and lubricants oils cannot be considered with a negligible mass. Therefore, the dynamics of the idealized system could not be replicated. With the implementation of the CB-TMD a proposal of geometric nonlinearities with elastic and viscous elements of negligible masses is presented. This is achieved due to the mass of the cables is very small in comparison with the rest of the structure.

It is assumed that CB-TMD can be used to attenuate the vibration of a structure that presents a linear vibration, this attenuation could be achieved in cases of free vibration and forced vibration. As a result of the behavior of geometrically nonlinear oscillations, a variation in the mass could decrease the settling time mainly upon resonance with the vibration of the first degree of freedom; also, vibratory amplitude of a structure due to a forced input could be reduced too. For this reason, a dynamic oscillatory system with two degrees of freedom has been designed and built. This test rig has the objective of validating the mathematical model experimentally.

doi: 10.18178/ijmerr.9.10.1371-1378

In section number 2 of this article, we describe the mathematical model by which the vibration of two degrees of freedom is interpreted. It considers the geometric nonlinearities of the cables. In section number 3, the design of the test rigs is used to validate the model is presented, and the specific features necessary to carry out precision measurements are discussed. Section 4 describes the procedures for validation experiments were carried out the. Consequently, in section number 5, the results of the numerical simulations in comparison with the experimental data are presented. Finally, in section number 6 the pertinent conclusions and the suggested future work are shown.

II. Mathematical Model

In this section, it is shown a dynamic discrete model of the dynamical system. The system has two degrees of freedom. The first degree of freedom corresponds to a linear oscillator with damping and stiffness; this is called the main structure. The second degree of freedom is a nonlinear oscillator; a system of wires in planar configuration was implemented. The stiffness and damping have geometrically induced nonlinear behavior, and is called the damper mass.

A. Geometric Nonlinearities

The geometric non linearities are due to the change in the direction of the cables during the vibration. The equivalent axial elasticity and viscosity of the cable is linear, but the change in the direction brings another behavior. Fig. 1 shows a diagram of the geometrically nonlinear oscillation.

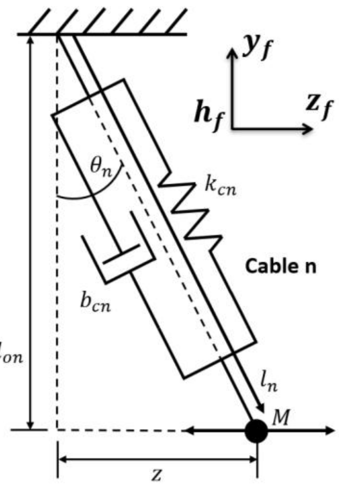

Figure 1. Diagram of the full dynamic model.

The forces in z_f direction of the described system is described as follows. The forces through the cable in all the moment are defined by f_{cn}; this is the sum of the spring f_{ckn} force and the pretention f_{ptn}.

$$f_{cn} = f_{ckn} + f_{ptn} \tag{1}$$

The main force is the spring force in z_f direction. This force is defined by

$$f_{kzn} = f_{cn}Sen(\theta_1) = (f_{ckn} + f_{ptn})Sen(\theta_1) \tag{2}$$

Where the force due to the elongation is

$$f_{kn} = k_{cn}(l_n - l_{on}) \tag{3}$$

The length of the spring in all the time is

$$l_n = \sqrt{{l_{on}}^2 + z^2} \tag{4}$$

Thus, the force due to the equivalent spring in the cable is a function of cable elongation. In all time, its value is

$$f_{kn} = k_{cn}\left(\sqrt{{l_{on}}^2 + z^2} - l_{on}\right) \tag{5}$$

The force in z_f direction due to just the spring is the vertical component of the previously defined force.

$$f_{kzn} = k_{cn}Sen(\theta_n)\left(\sqrt{{l_{on}}^2 + z^2} - l_{on}\right) \tag{6}$$

Incorporating the force of pretention, the equation has the following form.

$$f_{kzn} = Sen(\theta_n)\left[k_{cn}\left(\sqrt{{l_{on}}^2 + z^2} - l_{on}\right) + f_{ptn}\right] \tag{7}$$

The angles θ_n can be formulated through known variables in the system.

$$Sen(\theta_n) = \frac{z}{\sqrt{{l_{on}}^2 + z^2}} \tag{8}$$

Thus, the equation that defines the cable force due to a spring elongation and a pretention has the following form.

$$f_{kzn} = \frac{z}{\sqrt{{l_{on}}^2 + z^2}}\left[k_{cn}\left(\sqrt{{l_{on}}^2 + z^2} - l_{on}\right) + f_{ptn}\right] \tag{9}$$

After a simplification, the equation takes the following form.

$$F_{kzn} = \frac{z\left[f_{ptn} - k_{cn}\left(l_{on} - \sqrt{{l_{on}}^2 + z^2}\right)\right]}{\sqrt{{l_{on}}^2 + z^2}} \tag{10}$$

The development of the geometrically nonlinear damper is described as follow. The general expression of the force that generates to a damper in function to velocity is the following.

$$f_{bn} = b_{cn}\frac{dx}{dt} \tag{11}$$

The horizontal component of f_{bn}, this is in t z_f direction is presented in the following equation.

$$f_{bzn} = f_{cbn} \sin\theta_n = \left(b_{cn}\frac{dx}{dt}\right)\sin\theta_n \tag{12}$$

The coefficient must consider the geometric properties of the shock absorber in any position; therefore, the expression is as follows.

$$f_{bn} = b_{cn}\frac{dx}{dt} = b_{cn}\frac{z}{\sqrt{a^2+z^2}}\left(\frac{dz}{dt}\right) \tag{13}$$

The angles θ_n can be presented through variables known in the system.

$$Sen(\theta_n) = \frac{CA}{H} = \frac{z}{\sqrt{a^2+z^2}} \tag{14}$$

Finally, the full equation has the following form.

$$F_{bzn} = b_{cn}\left(\frac{z^2}{{l_{on}}^2+z^2}\right)\frac{dz}{dt} \tag{15}$$

Some authors have studied the geometrically nonlinear damping phenomenon [7], [8] y [9].

B. Full Dynamic Model

In Fig. 2 it is shown the dynamic diagram of the proposed system. The mass of the structure is represented by m_e, it is connected to mechanical ground through the linear spring k_e and the linear damper b_e. The second mass m_a is connected to the mass m_e through six steel cables, which are represented by the diagonal springs and dampers k_{c1}, b_{c1} and k_{c2}, b_{c2}. Each mass represents one degree of freedom that have a linear displacement in the z_f direction according to the reference frame h_f.

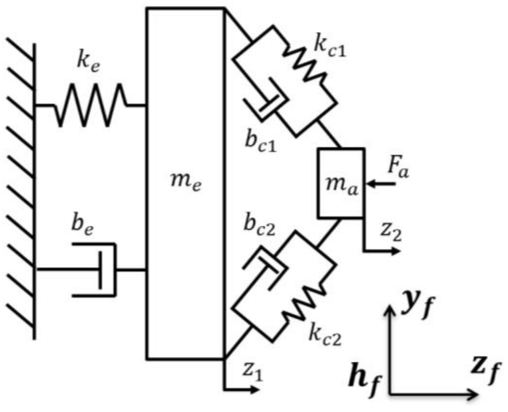

Figure 2. Diagram of the full dynamic model.

The equations of motion that define this model are shown below.

$$m_e\frac{d^2z_1}{dt^2} + b_e\frac{dz_1}{dt} + k_e z_1 + F_{kzA} + F_{kzB} + F_{bz} = 0 \tag{16}$$

$$m_a\frac{d^2z_2}{dt^2} + b_a\frac{dz_2}{dt} + f_{kzA} + f_{kzB} + f_{bz} = 0 \tag{17}$$

The terms $F_{kznA} + F_{kznB} + F_{bzn}$ represent the cable spring and damper force in z_f direction. These are the equations previously defined for the geometric nonlinearities of the cables.

$$F_{kzA} = \sum_{n=1}^{4} F_{kznA}$$

$$F_{kznA} = \frac{(z_1-z_2)}{\sqrt{{l_{on}}^2+(z_1-z_2)^2}}\left[f_{ptn} + T_w - k_{cn}\left(l_{on} - \sqrt{{l_{on}}^2+(z_1-z_2)^2}\right)\right] \tag{18}$$

$$F_{kzB} = \sum_{n=1}^{2} F_{kznB}$$

$$F_{kznB} = \frac{(z_1-z_2)}{\sqrt{{l_{on}}^2+(z_1-z_2)^2}}\left[f_{ptn} - k_{cn}\left(l_{on} - \sqrt{{l_{on}}^2+(z_1-z_2)^2}\right)\right] \tag{19}$$

$$F_{bz} = \sum_{n=1}^{6} F_{bzn}$$

$$F_{bzn} = b_{cn}\left(\frac{(z_1-z_2)^2}{{l_{on}}^2+(z_1-z_2)^2}\right)\left(\frac{dz_1}{dx} - \frac{dz_2}{dx}\right) \tag{20}$$

The terms $f_{kznA} + f_{kznA} + f_{bzn}$ are similar equations to the (18), (19) and (20) with some differences in terms of position and velocity, these equations are shown below.

$$f_{kzA} = \sum_{n=1}^{4} f_{kznA}$$

$$f_{kznA} = \frac{(z_2-z_1)}{\sqrt{{l_{on}}^2+(z_2-z_1)^2}}\left[f_{ptn} + T_w - k_{cn}\left(l_{on} - \sqrt{{l_{on}}^2+(z_2-z_1)^2}\right)\right] \tag{21}$$

$$f_{kznB} = \frac{(z_2-z_1)}{\sqrt{{l_{on}}^2+(z_2-z_1)^2}}\left[f_{ptn} - k_{cn}\left(l_{on} - \sqrt{{l_{on}}^2+(z_2-z_1)^2}\right)\right] \tag{22}$$

$$f_{bz} = \sum_{n=1}^{6} f_{bzn}$$

$$f_{bzn} = b_{cn}\left(\frac{(z_2 - z_1)^2}{{l_{on}}^2 + (z_2 - z_1)^2}\right)\left(\frac{dz_2}{dx} - \frac{dz_1}{dx}\right) \qquad (23)$$

The previous model considers the number of cables, the effect of the end effector weight T_w and the friction between the second degree of freedom and the air b_e.

III. Experimental Procedure

Experimentation consisted in evaluate the free and forced response of the first Degree of Freedom (1st dof or main structure) with the implementation of a second degree of freedom (2nd dof) with geometrical nonlinearities. The nonlinearities consist of an arrangement of cables in a planar configuration. To achieve this, a special test rig was built and characterized. A diagram set up of the experiment is shown in Fig. 3.

Firstly, free vibration was studied. The settling time was the parameter of interest in that test. The 1st dof settling time of the free vibration without a CB-TMD was compared with the 1st dof settling time of the free vibration implementing a 2nd dof, that is, the CB-TMD. Masses of 0.350-0.750-1.350 in CB-TMD were used for this comparison. Initial condition of 25 mm in both positions were set.

Secondly, forced vibration was studied. The vibratory amplitude of the stationary response was the parameter of interest in that test. The vibratory amplitude of the 1st dof without a CB-TMD was compared with the vibratory amplitude of the 1st dof implementing a 2nd dof, that is, the CB-TMD. The input force was 1.7 N and frequencies from 1 Hz to 3 Hz was used.

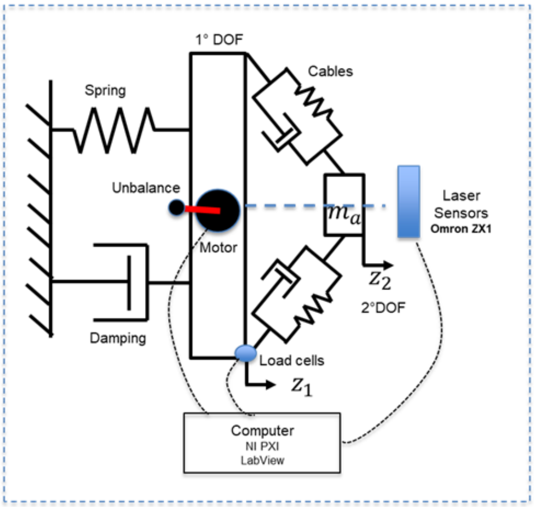

Figure 3. A block diagram of experimental set up

A photograph of the test rig is shown in Fig. 4. It was designed to study the response either free vibrations or forced vibrations of systems with a main linear structure, this is, the 1st dof. A 2nd dof with geometrical nonlinearities was designed to function as a CB-TMD. Some design principles were used on the test bench. These are kinematic design, direct application of forces, and minimal contact surfaces.

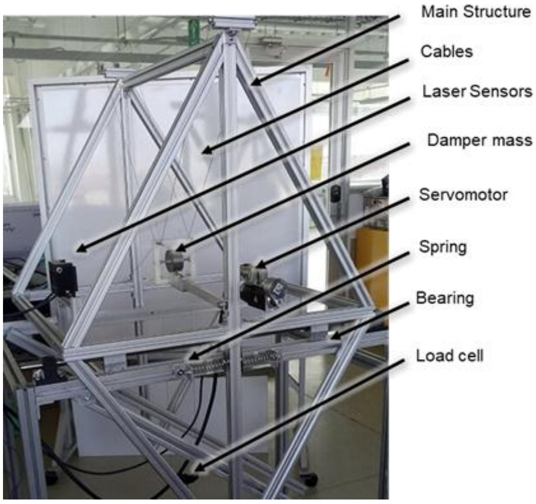

Figure 4. Test rig

A. Mechanical Integration of the Test Bench

A kinematic mechanical design was implemented to avoid over constraints in the displacement of the main structure. To ensure a soft displacement without undesirable blockages in the mechanism, a cylindrical joint was placed in one side of the linear displacement and in the other side a rolling joint was placed. This is shown in Fig. 5.

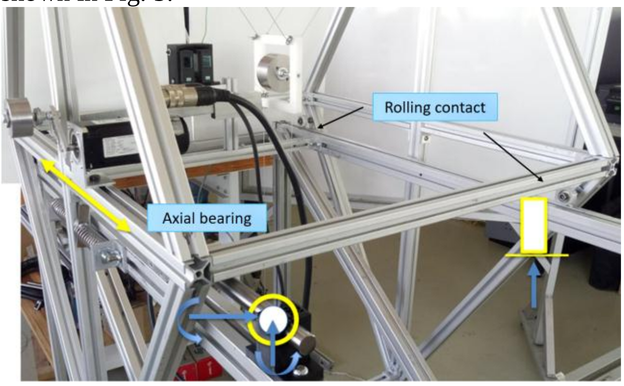

Figure 5. Kinematic design

The test bench table is made of aluminum profiles and rests firmly on the ground. The main structure or 1st gdl has a rhombus shape in order to increase its rigidity and be considered as a rigid solid. It is symmetrical to ensure that the center of mass coincides with the geometric center. It is made of aluminum profiles. Between the mechanical ground (table) and the 1st dof (main structure) there are the springs and the linear bearings.

The 2nd dof or CB-TMD is a polymer (PLA) structure that enable to change mass on a discrete manner. The way in which it is held by the cables decreases its sensitivity to rotations or translations in a direction other than z. The CB-TMD is joined to the main structure by cables, stress can be setting through a precision screw. This is shown in Fig. 6.

Figure 6. Laser sensors on main structure and 2 °dof

Forced forces are generated by a disbalanced rotor, it is actuated with a servo motor mounted in the main structure. This is shown in Fig. 7. The servo motor works to constant velocity controlled through a LabView interface. The rotation generates a centrifugal force sine as F=meω^2*sinωt. Since the point of view of the main structure there is a sinusoidal force in the z direction. Manipulation the parameters velocity of the motor, mass in the rotor and distance of these mass it is obtained different combinations of force and frequencies.

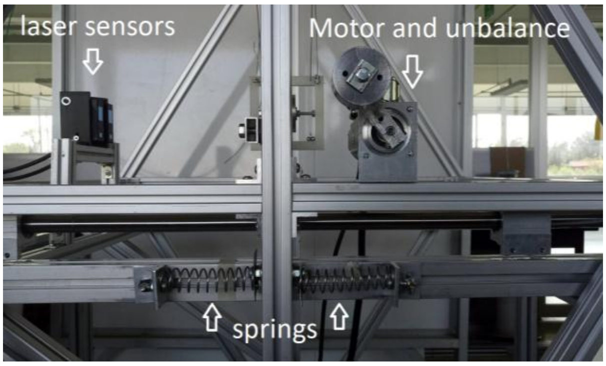

Figure 7. Components in test bench

Characterization of elements used in the test bench:

Spring: To obtain the spring stiffness constant, one extreme of the spring was fixed and the other was loaded with a set of different masses, the length change was measured. The spring used in the experiment has a linear behavior under the studied range.

Damper: Free vibration was used to obtain the main structure damping, it was displaced since equilibrium and released, displacement was measured and processed. Response was compared with known linear damping with viscous through a graphical method. Finally, value was adjusted to find damping coefficients. Main structure damping is present in springs and bearings.

Cables: Based on previous researches, cables were characterized through free vibrations. The axial viscoelasticity of the cables behaves like a kelvin-voigt model. Therefore, the characterized parameters were spring constant and viscosity. The spring and damping characteristics of the cable are a function of the cable length.

TABLE I. PARAMETERS USED IN THE TEST RIG

Parameter	Value
m_e	14.2 Kg
k_e	1540 N/m
b_e	18.5 N/(m/s)
m_a	0.375; 0.896; 1.35 kg
k_{c1}	30000 N/m
b_{c1}	100 N/(m/s)
pt	6 N
l_o	0.625 m
T_w	4.9135 N
b_a	0.01 N/(m/s)

B. Sensors and Instruments

Designed test rig uses two load cells and two displacement laser sensors. The load cells have a capacity of 15 kg and 3 kg, these were used to measure input forces of the 1 dof and to measure stress on cables respectively. Input force is measured between mechanical ground and main structure, while stress on cables are measured between 2 °DOF and the main structure. Displacement laser sensors have a range of measurement of 300 m and a resolution of 30 mm, these are used to measure displacement of each degree of freedom. These are fixed on mechanical ground.

We used an industrial computer NI PXIe-1082 with a controller NI PXIe-8135. There are two modules in the computer, one module of multiple purpose I/O model NI PXIe-6363 and a module of load cells model NI TB-4330. There are a Compact Rio 9030 that control a servo motor.

A human machine interface was programed in LabView® software, where the tests are executed and controlled. It has an interactive panel to view the force, displacements and cable stress, also settings for start and stop the test.

C. Procedure for Numerical Simulations

Computational numeric methods were used to simulate the dynamic models in a computer. In Matlab® software version R2019a there are schedule scripts which call functions of the dynamic models. The dynamical models were solved with default ode45 Matlab® function. It is used to solve nonlinear systems.

Frequency response simulation algorithm uses a sweep parameter methodology, one “for” cycles sweep the parameters for desired range of input frequency ω. The step for simulations were used to achieve legible graphics and describe the phenomenon. In each iteration, the amplitude and frequency of the signal is calculated and saved in a matrix, finally these values are plotted. A resume of the algorithm is shown in Fig. 8.

```
For (Minimum F to Maximum F)
    For (Minimum ω to Maximum ω)
        Run the simulation
        Get the amplitude of the signal
        Save the amplitude time in matrix1
        Get the frequency of the signal
        Save the frequency in a matrix2
 end
Graph surface (matrix1)
Graph surface (matrix2)
```

Figure 8. Algorithm for the optimization of the tuned mass damper.

Free vibration simulation algorithm uses a sweep parameter methodology, one "for" cycles sweep the parameters for desired range of input mass. Data were analyzed considered setting time to free vibrations. The default command step info in Matlab® was used to know steady-state response within the 5% of the final.

Data for frequencies response were analyzed as a function of the vibration's amplitude in the steady-state response, known maximum and minimum response values. We used defaults max and min Matlab® functions.

IV. Results

In this section, the mathematical model described in section II was simulated through numerical methods in Matlab® software. First a comparison between simulated and real free vibration of the first and second degree of freedom is presented. Then, the effectiveness of the CB-TMD is evaluated in the cases of free vibration and forced vibration. Evaluation criterion is the settling time in case of free vibration and the vibratory amplitude in the case of forced vibration.

A. Behaviour of Each Degree of Freedom

Fig. 9 shows the graph that represent real and simulated free vibration responses of the main structure, this is the first degree of freedom. The free vibration is due to an initial position condition of -30 mm. The black line is the simulated data and the blue line is the real data obtained through the test rig. It is observed that the real oscillation has a linear decrement in the amplitude while the simulated has an exponential decrement. This behavior could be due to Coulomb friction components in the main structure vibration m_e. Also settling time of the simulated vibration is 5.79 s and the settling time of the real structure is 5.85 s.

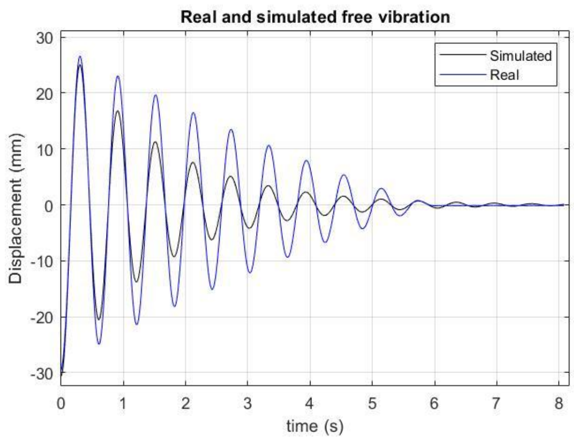

Figure 9. Comparison between real and simulated free vibration response of the main structure.

Fig 10 shows the graph that represent real and simulated free vibration responses of the damper mass, this is the second degree of freedom m_a. The free vibration is due to an initial position condition of 30 mm. The black line is the simulated data and the blue line is the real data obtained through the test rig. To make this test the main structure was fixed to mechanical ground so that the damper mass vibrates with reference to mechanical ground. It is observed that both graphs are similar. This kind of oscillation has a long settling time and a big amplitude. The internal viscous friction looks evident in its exponential decrement.

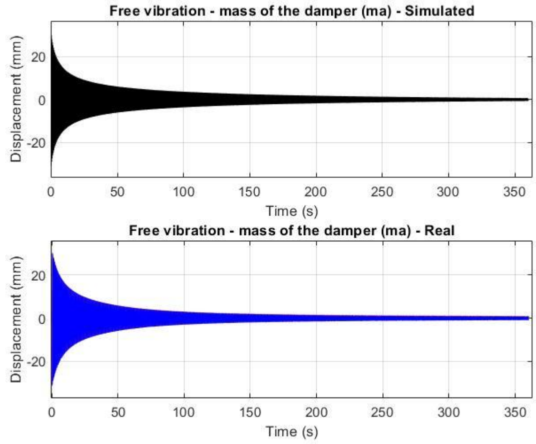

Figure 10. Comparison between the real and simulated free vibration response of damper mass.

B. Effectivness of the CB-TMD in the Free Vibrations

To evaluate the influence of CB-TMD in the settling time of the main structure m_e, simulations and validation experiments were carried out in the test rig. The mathematical model was simulated to evaluate the settling time of the structure with respect to different mass values. Subsequently, experimental validations were performed by varying the mass of the damper m_a in the test rig.

Fig. 11 shows the graph that represent in the black line the simulation for a variation of the mass of the damper m_a from 0.1 Kg to 1.5 Kg. The blue dots represent the real values obtained through experimentation. An increase in settling time is observed with respect to an increase in the mass of the damper m_a. The theoretical and experimental results were evaluated for an initial position condition of 25 mm.

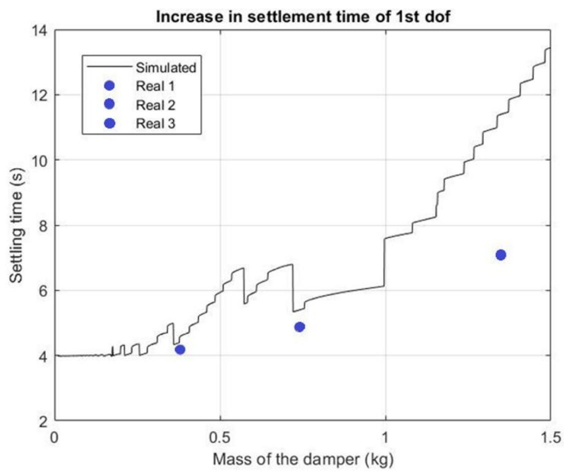

Figure 11. Comparison between the real and simulated free vibration response of damper mass.

Fig. 12 shows the graph that represent the response in time of the two degrees of freedom during a free vibration. The mass value of the damper was 0.896 kg. The blue line is the vibration of the main structure, the red line is the vibration of the damper mass. The graph shows real data generated with the test rig. It is appreciated the interaction between both displacements, the difference between the amplitudes and the discrepancy in settlement times. Due to the low energy dissipation characteristic of the second degree of freedom, it remains oscillating long time after the oscillation of the main structure has already stopped or settled.

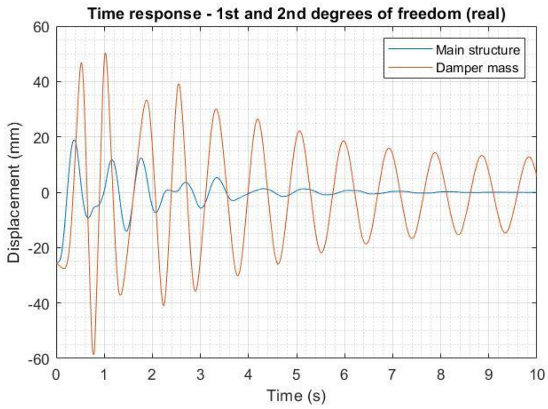

Figure 12. Response in time of the two degrees of freedom during a free vibration.

C. *Effectivness of the CB-TMD in the Forced Vibrations*

Fig. 13 shows real and simulated values of frequency response of the main structure. Two cases are presented, in black line the frequency vs. amplitude of the main structure without the use of CB-TMD and in red line the frequency against amplitude of the main structure with a CB-TMD. Black circles represent experimental measurements of vibrational amplitude without CB-TMD and red circles represent experimental measurements of the vibrational amplitude with CB-TMD.

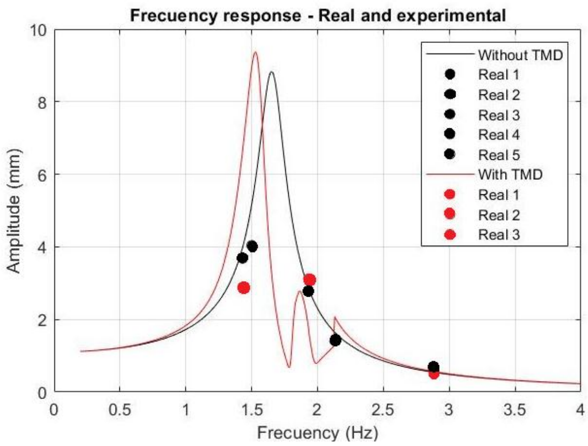

Figure 13. Real and simulated values of frequency response of the main structure

Fig. 14 shows the response in time of the two degrees of freedom during a forced vibration. The mass value of the damper was 0.896 kg. Both graphs show main structure vibration and correspond to the first degree of freedom. The blue line shows vibration without a CB-TMD, and the red line shows vibration with a CB-TMD. The graph shows real data that was generated using designed test rig. Differences in amplitude between both cases can be observed.

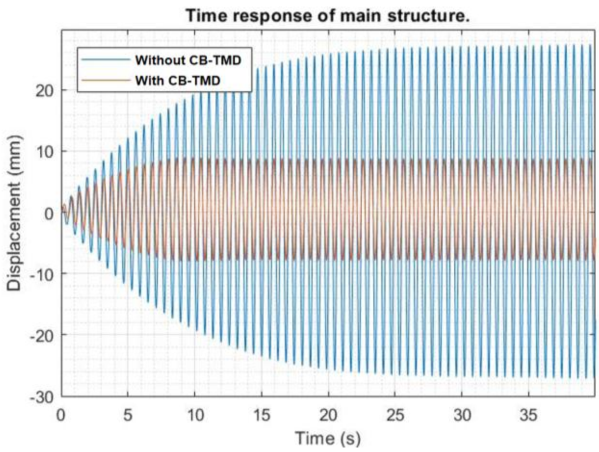

Figure 14. Response in time of the two degrees of freedom during a force vibration

V. Conclusions

In this investigation, the concept of cable-based tuned mass damper with geometric nonlinearities was presented, and the mathematical model of this system was developed. Its effectiveness to attenuate the vibration of a linear oscillatory system was evaluated numerically and experimentally. Specifically, its effectiveness was analyzed to decrease the settling time of the free vibration of a structure and to decrease the forced vibrational amplitude of the same structure. To achieve this, computer simulations of the mathematical model were performed. Subsequently, a test rig was built, dynamic parameters were characterized and experiments in free and forced vibration were performed in order to validate the mathematical model.

From the numerical and experimental observations, it is concluded that the cable-based tuned mass damper with geometric nonlinearities does not contribute in reducing settling time of the free vibrations of linear oscillations of a degree of freedom, contrary it presents an increase in settlement time. Based on the numerical and experimental evidence, this phenomenon is attributed to the increase in the potential energy of the system with the addition of the second degree of freedom, and to the zone of low energy dissipation presented by the geometrically non-linear oscillator.

From the behavior of the structural vibration due to a forced entry, it is concluded that the cable-based tuned mass damper with geometric non-linearities is viable for the reduction of the vibrational amplitude of the first degree of freedom. There is no great dissipative capacity in the tuned mass damper due to a low energy dissipation zone near the equilibrium point; therefore, the decrease in the first degree vibrational amplitude is due to resonant interference between the first and second degree of freedom, transmitting energy to the second degree of freedom.

The cable-based tuned mass damper with geometric nonlinearities is a concept whose advantages and disadvantages are still being evaluated. It is necessary to continue researching to explore its characteristics which are the areas of low rigidity and low energy dissipation centered on the equilibrium point. From the experience of the authors at the time of design and construction, some other advantages can be mentioned, which are a simple mechanical structure and fast implementation. It implies lower design, manufacturing and maintenance costs.

As a future work, it is suggested a study of the influence of other variables such as the length of the cables, the number of cables and the level of tension of the cables is suggested. As well as the research of the frequency response of the nonlinear oscillatory system as a 1st degree of freedom.

Conflict of Interest

The authors declare that there is no conflict of interest regarding the publication of this article.

Author Contributions

Alejandro C. Ramirez-Reivich and Ma. Del Pilar Corona-Lira conducted the research; Diego A. Zamora-Garcia made mathematical model and he analyzed the data; Luis M. Acosta-Carrion designed the test rig; Mercedes X. Zepeda-Fuentes made characterization of test rig and she collected experimental data. All authors wrote the paper and they had approved the final version.

Acknowledgment

The authors would like to recognize the support of the PAPIIT UNAM no. 102318 with the name “Investigación y análisis de la influencia del efecto de amortiguamiento electromagnético en la atenuación de vibraciones en sistemas actuados por tensores” and the support of the Mexican government through the CONACYT scholarship system.

References

[1] M. G. Soto and H. Adeli, "Tuned mass dampers," *Archives of Computational Methods in Engineering,* vol. 20, no. 4, pp. 419–431, 2013.

[2] A. J. Dick, A. Atzil, and S. Nagarajaiah, "Analytical investigation of vibration attenuation with a nonlinear tuned mass damper," in *Proc. the ASME 2015 International Mechanical Engineering Congress and Exposition,* Houston, 2015.

[3] L. Zuo and W. Cui, "Dual-functional energy-harvesting and vibration control: electromagnetic resonant shunt series tuned mass dampers," *Journal of Vibration and Acoustics,* vol. 135, 2013.

[4] D. A. Zamora-Garcia, A. C. Ramirez-Reivich, M. P. Corona-Lira, J. Eden and D. Oetomo, "On the use of tuned mass dampers for reducing the nonlinear vibrations of planar parallel cable robots," *International Journal of Mechanical Engineering and Robotics Research,* vol. 8, no. 3, pp. 406-412, 2019.

[5] D. A. Zamora-Garcia, L. M. Acosta-Carrion, M. P. Corona-Lira and A. C. Ramirez-Reivich, "Experimental determination of axial viscoelasticity of braided steel cables through the design of a special purpose machine," *ASME International Mechanical Engineering Congress and Exposition,* Salt Lake City, 2019.

[6] J. Dai, X. Zhao-Dong, and G. Pan-Pan, "Dynamic analysis of viscoelastic tuned mass damper system under harmonic excitation," *Journal of Vibration and Control,* vol. 25, pp. 1695-1706, 2019.

[7] B. Tang and M. Brennan, "A comparison of two nonlinear damping mechanisms in a vibration isolator," *Journal of Sound and Vibration,* no. 332, pp. 510-520, 2013.

[8] S. H. Nitzan, M. L. Valentina Zega, C. H. Ahn, A. Corigliano, T. W. Kenny, and D. A. Horsley, "Self-induced parametric amplification arising from nonlinear elastic coupling in gyroscope," *Scientific Reports,* pp. 1-6, 2015.

[9] J. C. Carranza, M. J. Brennan, and B. Tang, "Sources and propagation of nonlinearity in a vibration isolator with geometrically nonlinear damping," *Journal of Vibration and Acoustics,* vol. 138, 2016.

Diego A. Zamora-Garcia was born in Córdoba city, Mexico, on January 15th of 1990. He received the B.Eng. degree from the state university of Veracruz in 2012 and the Master’s in engineering from the National Autonomous University of Mexico in 2015, he is currently a Ph.D. candidate (mechanical engineering) from the National Autonomous University of Mexico.

He had participated in different projects of research and development at the center of advanced engineering at the National Autonomous University of Mexico. He is interested in mechatronic design and automation.

Luis M. Acosta-Carrion was born in Puerto la Cruz city, Venezuela, on January 10th of 1990. He received the B.Eng. degree from Simon Bolivar University in 2017 and he is currently a Master candidate (mechanical design) from the National Autonomous University of Mexico.

He had participated in different projects of research and development at the center of advanced engineering at the National Autonomous University of Mexico. He is interested in mechanical design.

Mercedes X. Zepeda-Fuentes was born in Mexico City, Mexico. She is currently a student of Mechanical Engineering from the National Autonomous University of Mexico.

She had participated in design projects at Center on Advanced Engineering at the National Autonomous University of Mexico. She is interested in the area of materials, manufacturing and design.

Ma. Del Pilar Corona-Lira was born in Mexico City, Mexico. She received the B.Eng. from the National Autonomous University of Mexico in 1992 and the Master of Science at Lancaster University in the United Kingdom in 1995. She received a Ph.D. from the National Autonomous University of Mexico in 2013.

She had developed new products integrating graduate and ungraduated students in its process. She has collaborated on several projects that involved multidisciplinary teams. She has taught different courses on electronics and mechatronics. She is interested in instrumentation, signal processing and surface inspection by Image processing.

Alejandro C. Ramirez-Reivich was born in Mexico City, Mexico. He received the B.Eng. from the National Autonomous University of Mexico in 1983 and the Master’s in engineering degree from the same institution in 1986. He received the Ph.D. degree at Lancaster University in the United Kingdom in 1995.

He had the opportunity to design new products together with graduate and ungraduated students. The integration and development of new manufacturing processes and make new systems for Mexican and foreign companies.